Robust Self-Supervised Learning with Lie Groups

Mark Ibrahim,* Diane Bouchacourt,* Ari Morcos

Fundamental AI Research (FAIR), Meta AI

Abstract

Deep learning has led to remarkable advances in computer vision. Even so, to-day's best models are brittle when presented with variations that differ even slightly from those seen during training. Minor shifts in the pose, color, or illumination of an object can lead to catastrophic misclassifications. State-of-the art models struggle to understand how a set of variations can affect different objects. We propose a framework for instilling a notion of how objects vary in more realistic settings. Our approach applies the formalism of Lie groups to capture continuous transformations to improve models' robustness to distributional shifts. We apply our framework on top of state-of-the-art self-supervised learning (SSL) models, finding that explicitly modeling transformations with Lie groups leads to substantial performance gains of greater than 10% for MAE on both known instances seen in typical poses now presented in new poses, and on unknown instances in any pose. We also apply our approach to ImageNet, finding that the Lie operator improves performance by almost 4%. These results demonstrate the promise of learning transformations to improve model robustness[1].

1   Introduction

State-of-the-art models have proven adept at modeling a number of complex tasks, but they struggle when presented with inputs different from those seen during training. For example, while classification models are very good at recognizing buses in the upright position, they fail catastrophically when presented with an upside-down bus since such images are generally not included in standard training sets (Alcorn et al., 2019). This can be problematic for deployed systems as models are required to generalize to settings not seen during training ("out-of-distribution (OOD) generalization"). One potential explanation for this failure of OOD generalization is that models exploit any and all correlations between inputs and targets. Consequently, models rely on heuristics that while effective during training, may fail to generalize, leading to a form of "supervision collapse" (Jo & Bengio, 2017; Ilyas et al., 2019; Doersch et al., 2020; Geirhos et al.,

---

*equal contribution

[1]Code to reproduce all experiments will be made available.

2020a). However, a number of models trained without supervision (self-supervised) have recently been proposed, many of which exhibit improved, but still limited OOD robustness (Chen et al., 2020; Hendrycks et al., 2019; Geirhos et al., 2020b).

The most common approach to this problem is to reduce the distribution shift by augmenting training data. Augmentations are also key for a number of contrastive self-supervised approaches, such as SimCLR (Chen et al., 2020). While this approach can be effective, it has a number of disadvantages. First, for image data, augmentations can only be applied to the pixels themselves, making it easy to, for example, rotate the entire image, but very difficult to rotate a single object within the image. Since many of the variations seen in real data cannot be approximated by pixel-level augmentations, this can be quite limiting in practice. Second, similar to adversarial training (Madry et al., 2017; Kurakin et al., 2016), while augmentation can improve performance on known objects, it often fails to generalize to novel objects (Alcorn et al., 2019). Third, augmenting to enable generalization for one form of variation can often harm the performance on other forms of variation (Geirhos et al., 2018; Engstrom et al., 2019), and is not guaranteed to provide the expected invariance to variations (Bouchacourt et al., 2021b). Finally, enforcing invariance is not guaranteed to provide the correct robustness that generalizes to new instances (as discussed in Section 2).

For these reasons, we choose to explicitly model the transformations of the data as transformations in the latent representation rather than trying to be invariant to it. To do so, we use the formalism of Lie groups. Informally, Lie groups are continuous groups described by a set of real parameters (Hall, 2003). While many continuous transformations form matrix Lie groups (e.g., rotations), they lack the typical structure of a vector space. However, Lie group have a corresponding vector space, their Lie algebra, that can be described using basis matrices, allowing to describe the infinite number elements of the group by a finite number of basis matrices. Our goal will be to learn such matrices to directly model the data variations.

To summarize, our approach structures the representation space to enable self-supervised models to generalize variation across objects. Since many naturally occurring transformations (e.g., pose, color, size, etc.) are continuous, we develop a theoretically-motivated operator, the *Lie operator*, that acts in representation space (see Fig. 1). Specifically, the Lie operator learns the continuous transformations observed in data as a vector space, using a set of basis matrices. With this approach, we make the following contributions:

1. We generate a novel dataset containing 3D objects in many different poses, allowing us to explicitly evaluate the ability of models to generalize to both known objects in unknown poses and to unknown objects in both known and unknown poses (Section 3).

2. Using this dataset, we evaluate the generalization capabilities of a number of standard models, including ResNet-50, ViT, MLP-Mixer, SimCLR, CLIP, VICReg, and MAE finding that all state-of-the-art models perform relatively poorly in this setting (Section 3.2).

3. We incorporate our proposed Lie operator in two recent SSL approaches: masked autoencoders (MAE, (He et al., 2021)), and Variance-Invariance-Covariance
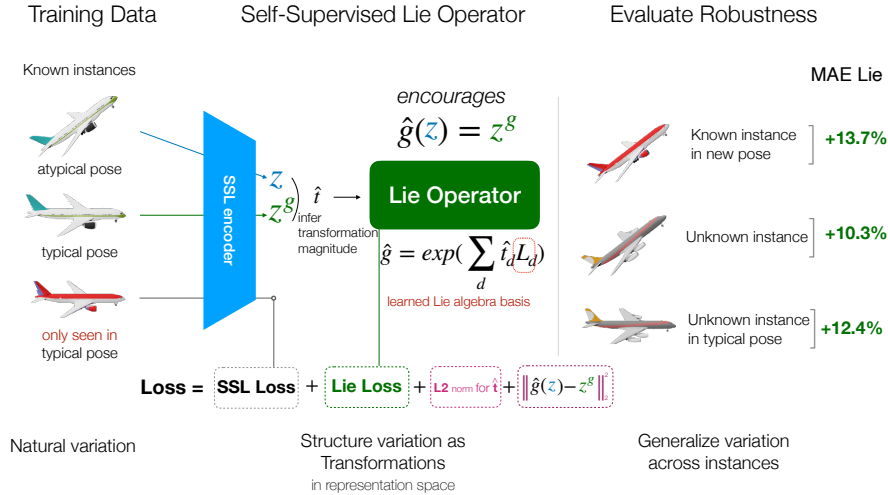
Figure 1: **Summary of approach and gains.** We generate a novel dataset containing rendered images of objects in typical and atypical poses, with some instances only seen in typical, but not atypical poses (left). Using these data, we augment SSL models such as MAE with a learned Lie operator which approximates the transformations in the latent space induced by changes in pose (middle). Using this operator, we improve performance by >10% for MAE for both known instances in new poses and unknown instances in both typical and atypical poses (right).

Regularization (VICReg (Bardes et al., 2021)) to directly model transformations in data (Section 2), resulting in *substantial OOD performance gains of greater than 10% for MAE* and of up to 8% for VICReg (Section 4.1). We also incorporate our Lie model in SimCLR (Chen et al., 2020) (Appendix E).

4. We run systemic ablations of each term of our learning objective in the MAE Lie model, showing the relevance of every component for best performance (Section 4.3).

5. We challenge our learned Lie operator by running evaluation on Imagenet as well as a rotated version of ImageNet, improving MAE performance by 3.94% and 2.62%, respectively. We also improve over standard MAE with MAE Lie when evaluated with finetuning on the iLab (Borji et al., 2016) dataset. These experiments show the applicability of our proposed Lie operator to realistic, challenging datasets (Section 5).

2   Methods

Humans recognize even new objects in all sorts of poses by observing continuous changes in the world. To mimic humans' ability to generalize variation, we propose a method for learning continuous transformations from data. We assume we have access

to pairs of data, e.g., images, $\mathbf{x}, \mathbf{x}'$ where $\mathbf{x}'$ is a transformed version of $\mathbf{x}$ corresponding to the same *instance*, e.g., a specific object, undergoing variations. This is a reasonable form of supervision which one can easily acquire from video data for example, where pairs of frames would correspond to pairs of transformed data, and has been employed in previous works such as Ick & Lostanlen (2020); Locatello et al. (2020); Connor et al. (2021b); Bouchacourt et al. (2021a).

Despite widespread use of such pairs in data augmentation, models still struggle to generalize across distribution shifts (Alcorn et al., 2019; Geirhos et al., 2018; Engstrom et al., 2019). To solve this brittleness, we take inspiration from previous work illustrating the possibility of representing variation via latent operators (Connor et al., 2021b; Bouchacourt et al., 2021a; Giannone et al., 2019). Acting in latent space avoids costly modifications of the full input dimensions and allows us to express complex operators using simpler latent operators. We learn to represent data variation explicitly as group actions on the model's representation space $\mathcal{Z}$. We use operators theoretically motivated by group theory, as groups enforce properties such as composition and inverses, allowing us to structure representations beyond that of an unconstrained network (such as an multi-layer perceptron, MLP) (see Appendix A). Fortunately, many common transformations can be described as groups.

We choose matrix Lie groups to model continuous transformations, as they can be represented as matrices and described by real parameters. However, they do not possess the basic properties of a vector space e.g., adding two rotation matrices does not produce a rotation matrix, without which back-propagation is not possible. For each matrix Lie group G however, there is a corresponding Lie algebra $\mathfrak{g}$ which is the tangent space of G at the identity. A Lie algebra forms vector space where addition is closed and where the space can be described using basis matrices. Under mild assumptions over G, any element of G can be obtained by taking the exponential matrix map: $\exp(t\mathbf{M})$ where $\mathbf{M}$ is a matrix in $\mathfrak{g}$, and t is a real number. Benefiting from the vector space structure of Lie algebras, we aim to learn a basis of the Lie algebra in order to represent the group acting on the representation space, using the $\exp$ map. We refer the reader to Appendix A and Hall (2003); Stillwell (2008) for a more detailed presentation of matrix Lie groups and their algebra.

2.1 Learning transformations from one sample to another via Lie groups

We assume that there exists a ground-truth group element, g, which describes the transformation in latent space between the embedding of $\mathbf{x}$ and $\mathbf{x}'$. Our goal is to approximate g using its Lie algebra. More formally, given a pair of samples (e.g., a pair of video frames), $\mathbf{x}$ and $\mathbf{x}'$, and an encoder, $f(\cdot)$, we compute the latent representations $\mathbf{z}$ and $\mathbf{z}^g$ as $\mathbf{z} = f(\mathbf{x})$ and $\mathbf{z}^g = f(\mathbf{x}')$. We therefore assume $\mathbf{z}^{\mathbf{g}} = f(\mathbf{x}') = g(f(\mathbf{x}))$. We aim to learn an operator $\hat{g}$ maximizing the similarity between $\mathbf{z}^{\hat{g}} = \hat{g}(f(\mathbf{x}))$ and $\mathbf{z}^g$.

We construct our operator by using the vector space structure of the group's Lie algebra $\mathfrak{g}$: we learn a basis of $\mathfrak{g}$ as a set of matrices $\mathbf{L_k} \in \mathbb{R}^{m \times m}, k \in \{1, \dots, d\}$ where d is the dimension of the Lie algebra and m is the dimension of the embedding space $\mathcal{Z}$. We use

this basis as a way to represent the group elements, and thus to model the variations that data samples undergo. A matrix $\mathbf{M}$ in the Lie algebra $\mathfrak{g}$ thus writes $\mathbf{M} = \sum_{k=1}^{d} t_k \mathbf{L_k}$ for some coordinate vector $\mathbf{t} = (t_1, \ldots, t_d) \in \mathbb{R}^d$.

Let us consider a pair $\mathbf{z}, \mathbf{z}^g$ with $\mathbf{z}^g = g(\mathbf{z})$. We assume the exponential map is surjective[2], thus, there exists $\sum_{k=1}^{d} t_k \mathbf{L_k} \in \mathfrak{g}$ such that

$$g = \exp(\sum_{k=1}^{d} t_k \mathbf{L_k}) = \exp(\mathbf{t}^\intercal \mathbf{L}) \tag{1}$$

where $\mathbf{t} = (t_1, \ldots, t_d)$ are the coordinates in the Lie algebra of the group element g, and $\mathbf{L}$ is the 3D matrix in $\mathbb{R}^{d \times m \times m}$ concatenating $\{\mathbf{L_k}, k \in \{1, \ldots, d\}\}$.

Our goal is to infer $\hat{g}$ such that $\hat{g}(\mathbf{z})$ (the application of the inferred $\hat{g}$ to the representation $\mathbf{z}$) equals $\mathbf{z}^g$. We denote $\mathbf{z}^{\hat{g}} = \hat{g}(\mathbf{z})$. Specifically, our transformation inference procedure consists of Steps 1-4 in Algorithm 1. For step 1 in Algorithm 1, similar to Connor et al. (2021b); Bouchacourt et al. (2021a), we use a pair of latent codes to infer the latent transformation. Additionally, we consider that we can access a scalar value, denoted $\delta_{x,x'}$, measuring "how much" the two samples differ. For example, considering frames from a given video, this would be the number of frames that separates the two original video frames $\mathbf{x}$ and $\mathbf{x}'$, and hence comes *for free*[3]. The coordinate vector corresponding to the pair $(\mathbf{z}, \mathbf{z}^g)$ is then inferred using a a multi-layer perceptron h[4]:

$$\hat{\mathbf{t}} = h(\mathbf{z}, \mathbf{z}^g, \delta_{\mathbf{x},\mathbf{x}'}) \tag{2}$$

When $\delta_{\mathbf{x},\mathbf{x}'}$ is small, we assume the corresponding images and embedding differ by a transformation close to the identity which corresponds to an infinitesimal $\hat{\mathbf{t}}$. To illustrate this, we use a squared L_2-norm constraint on $\hat{\mathbf{t}}$. For smaller $\delta_{\mathbf{x},\mathbf{x}'}$ (e.g., close-by frames in a video), larger similarity between $\mathbf{z}, \mathbf{z}^g$ is expected, in which case we want to encourage a smaller norm of $\hat{\mathbf{t}}$:

$$s(\mathbf{z}, \mathbf{z}^g, \delta_{\mathbf{x},\mathbf{x}'}) ||\hat{\mathbf{t}}||^2 \tag{3}$$

where $s : \mathcal{Z} \times \mathcal{Z} \times \mathbb{R} \to [0, 1]$ measures the similarity between $\mathbf{z}$ and $\mathbf{z}^g$. In our experiments, we simply use $s(\mathbf{z}, \mathbf{z}^g, \delta_{\mathbf{x},\mathbf{x}'})$ as a function of $\delta_{\mathbf{x},\mathbf{x}'}$ and compute

$$s(\delta_{\mathbf{x},\mathbf{x}'}) = \frac{1}{1 + \exp(|\delta_{\mathbf{x},\mathbf{x}'}|)}. \tag{4}$$

When $|\delta_{\mathbf{x},\mathbf{x}'}|$ decreases, s increases which strengthens the constraint in Eq. 3: the inferred vector of coordinates $\hat{\mathbf{t}}$ is therefore enforced to have small norm.

---

[2]This is the case if G is compact and connected (Hall, 2003, Corollary 11.10).

[3]Assuming that nearby video frames will be restricted to small transformations.

[4]During the learning of the parameters of h, we detach the gradients of the latent code $\mathbf{z}$ with respect to the parameters of the encoder f.

2.2 Lie learning objective

We encourage $\mathbf{z}^{\hat{g}}$ to be close to $\mathbf{z}^g$, while preventing a collapse mode where every transformation would be inferred as identity. In practice, recall we obtain $\mathbf{z}^g$ as the embedding $f(\mathbf{x}')$ of a corresponding frame. Specifically, we use an InfoNCE loss to match pairs[5]:

$$L_{\text{Lie}}(\mathbf{z}^{\hat{g}}, \mathbf{z}^g) = -\log \frac{\exp(sim(\mathbf{z}^{\hat{g}}, \mathbf{z}^g))}{\exp(sim(\mathbf{z}^{\hat{g}}, \mathbf{z}^g)) + \sum_{\tilde{\mathbf{z}} \in \mathcal{N}} \exp(sim(\tilde{\mathbf{z}}, \mathbf{z}^g))} \tag{5}$$

where sim is a similarity function measuring how close two latent embeddings are (e.g., cosine similarity in our experiments), and $\tilde{\mathbf{z}}$ belongs to set of negatives $\mathcal{N}$ for $\mathbf{z}^g$. For a given $\mathbf{z}^g$ of a given instance, the set $\mathcal{N}$ is comprised of latent codes of other instances. We also include other instances' transformed versions and their corresponding inferred transformed embeddings as negative samples.

Crucially, we also include in the negatives set of $\mathbf{z}^g$ (denoted $\mathcal{N}$) the frame encoding $\mathbf{z}$ in order to prevent the model from collapsing to a point where all the encodings of the same instance (i.e. any transformed version) would be mapped to the same point, and the inferred $\hat{g}$ would simply learned as identity. Indeed, one can view transformed pairs simply as another form of data augmentation, such that enforcing that $\mathbf{z}^g$ matches $\mathbf{z}$ (i.e. implicitly enforcing invariance) would bring robustness to the transformation g. However, we control for this in our experiments using the SimCLR model with our Lie operator (Appendix E, see SimCLR Frames baseline). We experiment with a baseline that is simply encouraged to match pairs of rotated frames in the representation, and SimCLR Lie outperforms this baseline. Thus, this shows that viewing transformations as data augmentation is not sufficient for robust generalization.

To further encourage $\mathbf{z}^g$ and $\mathbf{z}^{\hat{g}}$ to match, we add an Euclidean-type constraint:

$$\lambda_{\text{euc}} ||\mathbf{z}^g - \mathbf{z}^{\hat{g}}||^2 \tag{6}$$

The addition of the Euclidean loss helps to stabilize training, but using only the Euclidean loss (in place of our Lie loss) would not be enough to prevent the model from collapsing to mapping all transformed samples to the same point in latent space. Indeed, in the case of the MAE model, we perform ablations of our Lie model in Section 4.3 and show that all terms in the training objective are important for best performance with the MAE Lie model.

2.3 Learning a Lie operator in self-supervised representations

We use our Lie algebra model on top of two existing self-supervised (SSL) models, MAE and VICReg. In MAE, f is trained to reconstruct a masked input image, while VICReg is trained to match pairs of samples obtained from the same image via some form of data augmentations (e.g. two crops) and uses Variance-Invariance-Covariance regularization to prevent collapse. In Appendix E we also experiment applying our Lie

---

[5]Additionally, we forward the latent code through a neural projection head proj before computing similarity.

Algorithm 1: Implementing our Lie operator in a self-supervised learning model

    Input: x, x′

1 Encode $\mathbf{z} = f(\mathbf{x})$, $\mathbf{z}^g = f(\mathbf{x}')$ with the encoder f;

2 Infer $\hat{\mathbf{t}}$ as $\hat{\mathbf{t}} = h(\mathbf{z}, \mathbf{z}^g, \delta_{\mathbf{x},\mathbf{x}'})$;

3 Use the $\exp$ map to get $\hat{g} = \exp(\hat{\mathbf{t}}^\intercal \mathbf{L})$, where $\hat{g} \in \mathbb{R}^{m \times m}$;

4 Compute $\mathbf{z}^{\hat{g}} = \hat{g}(\mathbf{z})$. This is simple matrix-vector multiplication;

5 Jointly learn f, h, and $\mathbf{L}$ by minimizing:

$$\mathcal{L} = \lambda_{\text{ssl}}(L_{\text{ssl}}(\mathbf{z}) + L_{\text{ssl}}(\mathbf{z}^g)) + \lambda_{\text{lie}}L_{\text{Lie}}(\mathbf{z}^{\hat{g}}, \mathbf{z}^g) + \lambda_{\text{euc}}||\mathbf{z}^g - \mathbf{z}^{\hat{g}}||^2 + s(\delta_{\mathbf{x},\mathbf{x}'})||\hat{\mathbf{t}}||^2 \tag{8}$$

operator on the SimCLR (Chen et al., 2020) model, showing gains in the linear setting in particular. Our loss will balance between two components: the original SSL model loss L_{ssl}, applied to both samples of the pair separately, and the transformation loss L_{Lie}. Combining these constraints gives us our final loss, $\mathcal{L}$:

$$\mathcal{L} = \lambda_{\text{ssl}}(L_{\text{ssl}}(\mathbf{z}) + L_{\text{ssl}}(\mathbf{z}^g)) + \lambda_{\text{lie}}L_{\text{Lie}}(\mathbf{z}^{\hat{g}}, \mathbf{z}^g) + \lambda_{\text{euc}}||\mathbf{z}^g - \mathbf{z}^{\hat{g}}||^2 + s(\delta_{\mathbf{x},\mathbf{x}'})||\hat{\mathbf{t}}||^2 \tag{7}$$

The parameters λ_{ssl} and λ_{Lie} weight the two losses. Note that L_{ssl} can be different given the SSL model backbone we use. In our experiment we deploy our Lie operator on top of the Variance-Invariance-Covariance Regularization model (VICReg, (Bardes et al., 2021)), and of the very recent masked autoencoders model (MAE, (He et al., 2021)).

This loss is minimized with respect to the parameters of the encoder f, the parameters of the network h (multi-layer perceptron with two linear layers connected by a leaky ReLU) that infers the Lie algebra coordinates, and the Lie algebra basis matrices $\mathbf{L_k}$, $k \in \{1, \ldots, d\}$ which are used to compute $\hat{g}$. The total loss is over all the instances (N of them) and all possible pairs of transformed samples we have for each instance (if we have P pose changes, this will be $P(P-1)$). During training, we estimate this loss for a minibatch by sampling instances first, and sampling a pair of samples for each instance without replacement. The full procedure is illustrated in Fig. 1 and in Algorithm 1.

3   Evaluating generalization across instances

Our goal is to evaluate how well models generalize variation across instances. We focus on robustness to pose changes, a common, natural variation of objects. We evaluate the learned representations' robustness via standard linear evaluation or supervised finetuning protocols. Specifically, we measure classification top-1 accuracy across both *known* (seen during training) and *unknown instances* (not seen during training) in typical and

new poses. As only a portion of instances (less or equal to 50% in our experiments) are seen varying, motivated by works showing the benefit of data reweighting for generalization challenges (Idrissi et al., 2022), we sample data at training so that the model sees as many images varying as non varying by upsampling the varying instances where needed.

In order to perform well on known instances in new poses, models must learn to recognize an object regardless of its orientation and constitutes our weakest generalization test. In order to perform well on unknown instances, however, models must be able to generalize both across instances and poses, a substantially more difficult task.

3.1   Data variation

To conduct our evaluation, we develop a controlled dataset of common objects such as buses, cars, planes, etc. based on realistic object models from Trimble Inc [6]. We render nearly 500,000 images of varying 2D and 3D poses uniformly distributed with a step size of 4 degrees. To simulate natural changes in pose we organize pose changes temporally into frames (i.e. into images). Each frame captures a 4 degree change in pose either in-plane rotation or across all three axes. In addition, we conduct experiments evaluating the Lie operator on the iLab 2M dataset following the preprocessing steps from Madan et al. (2021).

3.2   Generalizing pose changes is challenging for SoTA vision models

We first assess state-of-the-art vision models' robustness to pose using a collection of supervised and self-supervised models (CLIP, ResNet-50, ViT-B/16, MLP Mixer, SimCLR, VICReg and MAE). All of these models rely on some form of data augmentation to provide invariance to nuisance features such as pose. We use ImageNet (Deng et al., 2009) pretrained embeddings for our models (with the exception of CLIP, which is pretrained on a large corpus of image-text pairs) (Radford et al.). We only show supervised linear evaluation for VICReg as it is mainly explored in the linear evaluation setting for the fully supervised task in Bardes et al. (2021).

While all models perform well on classification for known instances in typical poses, the same models have a considerable generalization gap to varying poses. In Figure 2, we show results for both linear evaluation and supervised finetuning classification gaps relative to typical poses of known instances. Strikingly, all models we evaluated exhibited large generalization gaps of 30-70% suggesting that even modern self-supervised models struggle to generalize both to new poses and to new instances. As such poor generalization can be problematic at best and dangerous at worst for deployed models, developing ways to improve generalization performance beyond simply augmenting the data is critical. In the next section, we introduce a new approach in which we encourage models not to be invariant to transformation, but rather to explicitly model and account for transformations.

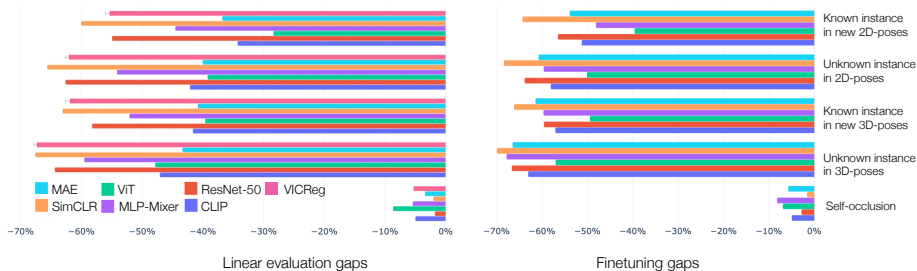
[6] freely available under a General Model license

Figure 2: **SoTA image classification models fail to generalize across poses and instances.** Bar plots show the gap in top-1 accuracy relative to training instances with poses seen during training. Self-occlusion is the gap in accuracy between unknown instances in 3D and 2D poses.

3.3 Incorporating a learned Lie operator in self-supervised learning models

To improve robustness, we incorporate a self-supervised learning phase where we structure representations using our Lie operator. During this phase, half of the instances are seen undergoing pose changes in 2D and 3D. We use the angle difference between frames as an proxy for frame distance (denoted δ in Section 2.1). In the case of rotation around all axes, we use the mean of three angles. We then evaluate the representations in the same manner as described above.

We implement our Lie operator in two SSL models: Masked Autoencoder (MAE) and Variance-Invariance-Covariance Regularization (VICReg). VICReg is a SSL method, which encourages similar representations among two views (generated via data augmentation) of an image. MAE is an SSL model whose learning objective is based on the reconstruction of a randomly masked input.

4 Results

4.1 SSL models with Lie operators are more robust across instances and poses

We evaluate the robustness benefits of our Lie operator across several generalization settings. In Figure 3, we plot the performance of a MAE (**A**) and VICReg (**B**) models with and without our Lie operator. Encouragingly, we find explicitly modeling transformations with Lie groups (referred to as MAE Lie and VICReg Lie) improves robustness for all generalization settings. For known instances (those seen during training), incorporating our Lie operator improves Top-1 classification accuracy for new poses by 13.7% for MAE Lie and 7.7% for VICReg Lie. In the more challenging settings of unknown instances which are never seen during training, we still observe performance gains for VICReg Lie of 0.2% for new instances in typical and 1.2% for those in new poses. For MAE Lie, we observe substantial performance gains of 12.4% for unknown instances in typical poses and 10.3% for those in diverse poses. We note both MAE and VICReg
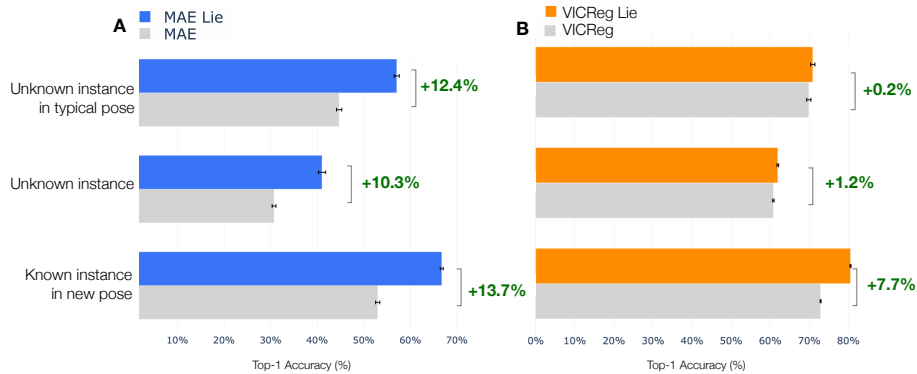
Figure 3: **Incorporating our Lie operator to MAE and VICReg improves generalization across poses and instances.** Bars indicate the mean top-1 accuracy and brackets indicating the standard error across seeds. In A., we show supervised finetuning for MAE Lie versus a standard MAE. In B., we show supervised linear evaluation for VICReg Lie versus VICReg as the original VICReg model is mainly explored in the linear evaluation setting for the fully supervised task (Bardes et al., 2021).

Lie bring even more substantial gains for settings when data diversity is limited (see Sec. 4.2 Tables 1 and 2).

4.2 Lie operator robustness gains are sustained even with limited diverse data

For our experiments so far, models have been exposed to a 50/50 mix of typical and atypical poses during supervised linear classification and finetuning. However, we want models to generalize across instances and to atypical poses even when presented with comparatively small amounts of diverse data. We therefore evaluated our models by performing supervised linear classification and finetuning with either 50%, 25%, or 5% of data featuring atypical poses (Tables 1 and 2). Notably, we observed that while overall performance decreased with fewer diverse instances, as we might expect, the relative gains of the Lie models were largely consistent across settings, and if anything, were larger for settings with less diverse data. These results demonstrate the robustness of our approach to differing quantities of diverse data.

4.3 Ablations

In Table 2, compared to our MAE Lie, a model with only the SSL term (and no Euclidean or Lie loss), that is, the baseline MAE, suffers drops of $10.3\%, 9.4\%$, and 8.2% in top-1 accuracy on unknown instances, respectively for the $5\%, 25\%$ and 50% diversity settings.

Table 1: **Assessing linear evaluation robustness to pose changes as the proportion of diverse instances seen during training varies.** Table reports linear evaluation top-1 accuracy as **mean** $\pm$ standard error (+ absolute difference, x relative multiple) to the baseline model.

diverse proportion top-1 accuracy (%)	known instance in new pose			unknown instance		
	5%	25%	50%	5%	25%	50%
VICReg Lie	**73.8 ± 0.2 (+14.4, 1.24x)**	**75.0 ± 0.0 (+5.8, 1.08x)**	**80.5 ± 0.1 (+7.7, 1.11x)**	**54.1 ± 0.2 (+3.7, 1.07x)**	**59.7 ± 0.1 (+3.1, 1.05x)**	**62.0 ± 0.2 (+1.2, 1.02x)**
VICReg	59.4 ± 0.0	69.1 ± 0.1	72.9 ± 0.1	50.4 ± 0.1	56.7 ± 0.2	60.8 ± 0.2
MAE Lie	**13.0 ± 0.2 (+1.3, 1.11x)**	**13.3 ± 0.4 (+2.3, 1.21x)**	**16.5 ± 0.3 (+4.1, 1.33x)**	**11.9 ± 0.5 (+1.2, 1.12x)**	**11.5 ± 0.2 (+1.2, 1.11x)**	**12.9 ± 0.4 (+1.3, 1.11x)**
MAE	11.6 ± 0.2	11.0 ± 0.4	12.4 ± 0.1	10.6 ± 0.2	10.3 ± 0.4	11.6 ± 0.5

Table 2: **Assessing finetuning robustness to pose changes as the proportion of diverse instances seen during training varies.** Table reports finetuning Top-1 Accuracy as **mean** $\pm$ standard error (+ absolute difference, x relative multiple) to the baseline model. We do not experiment with VICReg finetuning as the original paper (Bardes et al., 2021) focuses on linear evaluation.

diverse proportion top-1 accuracy (%)	known instance in new pose			unknown instance		
	5%	25%	50%	5%	25%	50%
MAE Lie	**49.2 ± 0.5 (+10.9, 1.28x)**	**60.4 ± 0.0 (+12.6, 1.26x)**	**66.7 ± 0.3 (+13.7, 1.26x)**	**28.4 ± 0.1 (+8.2, 1.40x)**	**36.6 ± 0.1 (+9.4, 1.35x)**	**41.0 ± 0.8 (+10.3, 1.34x)**
MAE	38.3 ± 0.5	47.8 ± 0.4	53.0 ± 0.5	20.2 ± 0.1	27.2 ± 0.3	30.7 ± 0.4

In addition, we ran systematic ablations for each loss component in our MAE Lie model. We find a consistent decrease in performance across all three diversity settings. Compared to our MAE Lie model, a model without the Euclidean loss term ($\lambda_{\text{euc}} = 0$) suffers drops of 10.5%, 9.08%, and 3.9% in top-1 accuracy for unknown instances (when 50%, 25%, or 5% of instances vary in pose during training, respectively). Similarly, compared to our MAE Lie, a model with only the Lie loss (i.e. $\lambda_{\text{euc}} = \lambda_{\text{ssl}} = 0$) suffers a drop of 5.9%, 5.01%, and 1.99% in top-1 accuracy for unknown instances across the three diversity settings. This result illustrates how each loss term is critical to the overall performance of our proposed MAE Lie model.

5 MAE Lie transfer on real objects datasets

5.1 ImageNet, Rot ImageNet

Table 3: **Results comparing MAE Lie versus MAE Top-1 Accuracy for ImageNet, Rot ImageNet (random rotations)** after finetuning of 20k steps on the ImageNet training set.

Top-1 Accuracy (%)	ImageNet Validation	Rot ImageNet Validation
MAE	63.61	34.50
MAE Lie	**67.55 (+3.94%)**	**37.12 (+2.62%)**

In order to further demonstrate the benefit of our proposed Lie operator to standard benchmarks, we perform evaluation on ImageNet (Deng et al., 2009) and some of its variants. Rot ImageNet consists of the same validation images on which we apply random rotations to assess how well models handle pose changes. To do so, we

finetune both the baseline MAE model and MAE Lie for 20k steps on ImageNet with a linear classification head. Table 3 reports the performance on the ImageNet and Rot ImageNet validation sets. We find MAE Lie outperforms the baseline for rotated ImageNet validation images by a considerable $+2.62\%$ in top-1 accuracy and the unaltered ImageNet validation set (by $+3.94\%$ in top-1 accuracy) which contain pose along with other changing factors. Details on the training can be found in Appendix B.1.3.

5.2 iLab dataset

To demonstrate the applicability of our approach to other datasets, we also evaluate our MAE Lie model on the iLab 2M dataset. The iLab 2M dataset (Borji et al., 2016) is a natural image dataset consisting of 2M images of toy objects, from multiple categories, undergoing variations in object instances, viewpoints, lighting conditions, and backgrounds. We follow the preprocessing steps in Madan et al. (2021). We partition the training samples into a validation set (10%) and show results on the iLab test set. We conduct supervised finetuning, the standard evaluation protocol for MAE. We observe MAE Lie yields nearly a 3% improvement on the test set ($93.2\% \pm 0.45\%$ MAE Lie vs $90.6\% \pm 0.11\%$ MAE) without re-training our Lie operator on the iLab dataset.

6 Related Work

Modeling variation Existing domain adaptation works (Zhou et al., 2020; Robey et al., 2021; Nguyen et al., 2021) learn transformations that map one domain to the other. In contrast to Ick & Lostanlen (2020); Hashimoto et al. (2017), we learn transformations in the latent space rather than image-space. Connor & Rozell (2020); Connor et al. (2021a) learn transformations in the latent space but uses a decoder that performs image reconstruction, which is known to be hard to apply to complex, large scale image data. In the context of classification, Benton et al. (2020) use the Lie algebra formalism to learn augmentations, but they require a priori knowledge of the augmentations. Tai et al. (2019) provides invariance to continuous transformations, but they only experiment on small scale data (MNIST (LeCun et al., 2010) and SVHN (Netzer et al., 2011)). We also depart from their work as we explicitly focus on the challenge of robustness to distributional shifts. Equivariant models (see Cohen & Welling (2016); Cohen et al. (2020) among others) and disentanglement (Higgins et al., 2018; Giannone et al., 2019) also aim to structure latent representations, but are mainly applied to synthetic, small scale data. Disentanglement also often requires costly pixel reconstruction. Spatial Transformer Networks (Jaderberg et al.) learn an instance-dependent affine transform for classification, resulting in behavior such as zooming in on the foreground object. Our goal differs as we focus on the generalization capabilities of various models to pose changes. Capsule networks (Sabour et al., 2017; Mazzia et al., 2021) were designed to better generalize to novel views, however, it is difficult for us to compare our approach to these as we require a strong pre-trained image model. To our knowledge, no such model using capsule networks exists, making a fair comparison very difficult.

OOD Generalization failures Alcorn et al. (2019); Engstrom et al. (2019) shed light on the failures of SoTA models on "unusual" examples that slightly vary from the training data, and Engstrom et al. (2019); Azulay & Weiss (2019) show that explicitly augmenting the data with such variations does not fix the problem. Indeed, Bouchacourt et al. (2021b) found that data augmentation does not bring the expected invariance to transformations, and that invariance rather comes from the data itself. Self-supervised models trained with InfoNCE theoretically recover the true data factors of variations (Zimmermann et al., 2021; von Kügelgen et al., 2021), but our experiments show that they do not generalize to distributional shifts.

7 Discussion

We aim to improve the OOD generalization of SSL models by encouraging them to explicitly model transformations using Lie groups. Using a novel dataset to evaluate OOD generalization, we found that applying our Lie operator to MAE and VICReg leads to markedly improved performance for both models, enabling better generalization both across poses and instances, both on our synthetic data and on ImageNet and its variations for MAE. Our results highlight that data augmentation alone is not enough to enable effective generalization and that structuring operators to explicitly account for transformations is a promising approach to improving robustness. We focus on modeling pose changes, a common natural factor of variation in objects. However, Lie groups are capable of describing a variety of naturally occurring continuous transformations. Future work could extend the application of Lie operators to these settings, possibly even to model multiple factors of variation at once.

Acknowledgements

References

Michael A. Alcorn, Qi Li, Zhitao Gong, Chengfei Wang, Long Mai, Wei-Shinn Ku, and Anh Nguyen. Strike (with) a pose: Neural networks are easily fooled by strange poses of familiar objects. 2019. URL http://arxiv.org/abs/1811.11553.

Aharon Azulay and Yair Weiss. Why do deep convolutional networks generalize so poorly to small image transformations? *Journal of Machine Learning Research*, 20(184):1–25, 2019. URL http://jmlr.org/papers/v20/19-519.html.

Adrien Bardes, Jean Ponce, and Yann LeCun. VICReg: Variance-invariance-covariance regularization for self-supervised learning. 2021. URL http://arxiv.org/abs/2105.04906.

Gregory Benton, Marc Finzi, Pavel Izmailov, and Andrew G Wilson. Learning invariances in neural networks from training data. In H. Larochelle, M. Ranzato, R. Hadsell, M. F. Balcan, and H. Lin (eds.), *Advances in Neural Information Processing Systems*, volume 33, pp. 17605–17616. Curran Associates, Inc., 2020. URL https://proceedings.neurips.cc/paper/2020/file/cc8090c4d2791cdd9cd2cb3c24296190-Paper.pdf.

Ali Borji, Saeed Izadi, and Laurent Itti. ilab-20m: A large-scale controlled object dataset to investigate deep learning. In *2016 IEEE Conference on Computer Vision and Pattern Recognition (CVPR)*, pp. 2221–2230, 2016. doi: 10.1109/CVPR.2016.244.

Diane Bouchacourt, Mark Ibrahim, and Stéphane Deny. Addressing the topological defects of disentanglement via distributed operators. *CoRR*, abs/2102.05623, 2021a. URL https://arxiv.org/abs/2102.05623.

Diane Bouchacourt, Mark Ibrahim, and Ari S. Morcos. Grounding inductive biases in natural images: invariance stems from variations in data. In A. Beygelzimer, Y. Dauphin, P. Liang, and J. Wortman Vaughan (eds.), *Advances in Neural Information Processing Systems*, 2021b. URL https://openreview.net/forum?id=p7GujbewmRY.

Ting Chen, Simon Kornblith, Mohammad Norouzi, and Geoffrey Hinton. A simple framework for contrastive learning of visual representations. 2020. URL http://arxiv.org/abs/2002.05709.

Taco Cohen and Max Welling. Group equivariant convolutional networks. In Maria Florina Balcan and Kilian Q. Weinberger (eds.), *Proceedings of The 33rd International Conference on Machine Learning*, volume 48 of *Proceedings of Machine Learning Research*, pp. 2990–2999, New York, New York, USA, 20–22 Jun 2016. PMLR. URL http://proceedings.mlr.press/v48/cohenc16.html.

Taco Cohen, Mario Geiger, and Maurice Weiler. A General Theory of Equivariant CNNs on Homogeneous Spaces. *arXiv:1811.02017 [cs, stat]*, January 2020. URL http://arxiv.org/abs/1811.02017. arXiv: 1811.02017.

Marissa Connor and Christopher Rozell. Representing closed transformation paths in encoded network latent space. In *The Thirty-Fourth AAAI Conference on Artificial Intelligence, AAAI 2020, The Thirty-Second Innovative Applications of Artificial Intelligence Conference, IAAI 2020, The Tenth AAAI Symposium on Educational Advances in Artificial Intelligence, EAAI 2020, New York, NY, USA, February 7-12, 2020*, pp. 3666–3675. AAAI Press, 2020. ISBN 978-1-57735-823-7. URL https://aaai.org/ojs/index.php/AAAI/article/view/5775.

Marissa Connor, Kion Fallah, and Christopher Rozell. Learning identity-preserving transformations on data manifolds. *CoRR*, abs/2106.12096, 2021a. URL https://arxiv.org/abs/2106.12096.

Marissa C. Connor, Gregory H. Canal, and Christopher J. Rozell. Variational autoencoder with learned latent structure. 2021b. URL http://arxiv.org/abs/2006.10597.

Jia Deng, Wei Dong, Richard Socher, Li-Jia Li, Kai Li, and Li Fei-Fei. Imagenet: A large-scale hierarchical image database. In *2009 IEEE conference on computer vision and pattern recognition*, pp. 248–255. Ieee, 2009.

Carl Doersch, Ankush Gupta, and Andrew Zisserman. Crosstransformers: spatially-aware few-shot transfer. In H. Larochelle, M. Ranzato, R. Hadsell, M.F. Balcan, and H. Lin (eds.), *Advances in Neural Information Processing Systems*, volume 33, pp. 21981–21993. Curran Associates, Inc., 2020. URL https://proceedings.neurips.cc/paper/2020/file/fa28c6cdf8dd6f41a657c3d7caa5c709-Paper.pdf.

Logan Engstrom, Brandon Tran, Dimitris Tsipras, Ludwig Schmidt, and Aleksander Madry. Exploring the landscape of spatial robustness. In Kamalika Chaudhuri and Ruslan Salakhutdinov (eds.), *Proceedings of the 36th International Conference on Machine Learning*, volume 97 of *Proceedings of Machine Learning Research*, pp. 1802–1811. PMLR, 09–15 Jun 2019. URL https://proceedings.mlr.press/v97/engstrom19a.html.

R. Geirhos, J.-H. Jacobsen, C. Michaelis, R. Zemel, W. Brendel, M. Bethge, and F. A. Wichmann. Shortcut learning in deep neural networks. *Nature Machine Intelligence*, 2(11):665–673, 2020a. doi: 10.1038/s42256-020-00257-z.

Robert Geirhos, Carlos R. M. Temme, Jonas Rauber, Heiko H. Schütt, Matthias Bethge, and Felix A. Wichmann. Generalisation in humans and deep neural networks. In S. Bengio, H. Wallach, H. Larochelle, K. Grauman, N. Cesa-Bianchi, and R. Garnett (eds.), *Advances in Neural Information Processing Systems*, volume 31. Curran Associates, Inc., 2018. URL https://proceedings.neurips.cc/paper/2018/file/0937fb5864ed06ffb59ae5f9b5ed67a9-Paper.pdf.

Robert Geirhos, Kantharaju Narayanappa, Benjamin Mitzkus, Matthias Bethge, Felix A. Wichmann, and Wieland Brendel. On the surprising similarities between supervised and self-supervised models. In *NeurIPS 2020 Workshop SVRHM*, 2020b. URL https://openreview.net/forum?id=q2ml4CJMHAx.

Giorgio Giannone, Jonathan Masci, and Christian Osendorfer. No representation without transformation. *CoRR*, abs/1912.03845, 2019. URL http://arxiv.org/abs/1912.03845.

B.C. Hall. *Lie Groups, Lie Algebras, and Representations: An Elementary Introduction*. Graduate Texts in Mathematics. Springer, 2003. ISBN 9780387401225. URL https://books.google.com/books?id=m1VQi8HmEwcC.

Tatsunori B Hashimoto, Percy S Liang, and John C Duchi. Unsupervised transformation learning via convex relaxations. In I. Guyon, U. V. Luxburg, S. Bengio, H. Wallach, R. Fergus, S. Vishwanathan, and R. Garnett (eds.), *Advances in Neural Information Processing Systems*, volume 30. Curran Associates, Inc., 2017.

Kaiming He, Xinlei Chen, Saining Xie, Yanghao Li, Piotr Dollár, and Ross Girshick. Masked autoencoders are scalable vision learners. 2021. URL http://arxiv.org/abs/2111.06377.

Dan Hendrycks, Mantas Mazeika, Saurav Kadavath, and Dawn Song. Using self-supervised learning can improve model robustness and uncertainty. In H. Wallach, H. Larochelle, A. Beygelzimer, F. d'Alché-Buc, E. Fox, and R. Garnett (eds.), *Advances in Neural Information Processing Systems*, volume 32. Curran Associates, Inc., 2019. URL https://proceedings.neurips.cc/paper/2019/file/a2b15837edac15df90721968986f7f8e-Paper.pdf.

Irina Higgins, David Amos, David Pfau, Sebastien Racaniere, Loic Matthey, Danilo Rezende, and Alexander Lerchner. Towards a Definition of Disentangled Representations. *arXiv:1812.02230 [cs, stat]*, December 2018. URL http://arxiv.org/abs/1812.02230. arXiv: 1812.02230.

Chris Ick and Vincent Lostanlen. Learning a lie algebra from unlabeled data pairs. volume abs/2009.09321, 2020. URL https://arxiv.org/abs/2009.09321.

Badr Youbi Idrissi, Martin Arjovsky, Mohammad Pezeshki, and David Lopez-Paz. Simple data balancing achieves competitive worst-group-accuracy. In *First Conference on Causal Learning and Reasoning*, 2022. URL https://openreview.net/forum?id=cDxT7WYhaD.

Andrew Ilyas, Shibani Santurkar, Dimitris Tsipras, Logan Engstrom, Brandon Tran, and Aleksander Madry. Adversarial examples are not bugs, they are features. In H. Wallach, H. Larochelle, A. Beygelzimer, F. d'Alché-Buc, E. Fox, and R. Garnett (eds.), *Advances in Neural Information Processing Systems*, volume 32. Curran Associates, Inc., 2019. URL https://proceedings.neurips.cc/paper/2019/file/e2c420d928d4bf8ce0ff2ec19b371514-Paper.pdf.

Max Jaderberg, Karen Simonyan, Andrew Zisserman, and Koray Kavukcuoglu. Spatial transformer networks. URL http://arxiv.org/abs/1506.02025.

Jason Jo and Yoshua Bengio. Measuring the tendency of cnns to learn surface statistical regularities. *CoRR*, abs/1711.11561, 2017. URL http://arxiv.org/abs/1711.11561.

Alexey Kurakin, Ian Goodfellow, and Samy Bengio. Adversarial machine learning at scale. *arXiv preprint arXiv:1611.01236*, 2016.

Yann LeCun, Corinna Cortes, and CJ Burges. Mnist handwritten digit database. *ATT Labs [Online]. Available: http://yann.lecun.com/exdb/mnist*, 2, 2010.

F. Locatello, B. Poole, G. Rätsch, B. Schölkopf, O. Bachem, and M. Tschannen. Weakly-supervised disentanglement without compromises. In *Proceedings of the 37th International Conference on Machine Learning (ICML)*, volume 119 of *Proceedings of Machine Learning Research*, pp. 6348–6359. PMLR, July 2020. URL http://proceedings.mlr.press/v119/locatello20a/locatello20a.pdf.

Spandan Madan, Timothy Henry, Jamell Dozier, Helen Ho, Nishchal Bhandari, Tomotake Sasaki, Frédo Durand, Hanspeter Pfister, and Xavier Boix. When and how CNNs generalize to out-of-distribution category-viewpoint combinations. 2021. URL http://arxiv.org/abs/2007.08032.

Aleksander Madry, Aleksandar Makelov, Ludwig Schmidt, Dimitris Tsipras, and Adrian Vladu. Towards deep learning models resistant to adversarial attacks. *arXiv preprint arXiv:1706.06083*, 2017.

Vittorio Mazzia, Francesco Salvetti, and Marcello Chiaberge. Efficient-capsnet: capsule network with self-attention routing. *Scientific reports*, 11, 2021.

Yuval Netzer, Tao Wang, Adam Coates, Alessandro Bissacco, Bo Wu, and Andrew Y. Ng. Reading digits in natural images with unsupervised feature learning. In *NIPS Workshop on Deep Learning and Unsupervised Feature Learning 2011*, 2011. URL http://ufldl.stanford.edu/housenumbers/nips2011_housenumbers.pdf.

A. Tuan Nguyen, Toan Tran, Yarin Gal, and Atilim Gunes Baydin. Domain invariant representation learning with domain density transformations. In *Thirty-Fifth Conference on Neural Information Processing Systems*, 2021. URL https://openreview.net/forum?id=l3vp7IDY6PZ.

Alec Radford, Jong Wook Kim, Chris Hallacy, Aditya Ramesh, Gabriel Goh, Sandhini Agarwal, Girish Sastry, Amanda Askell, Pamela Mishkin, Jack Clark, Gretchen Krueger, and Ilya Sutskever. Learning transferable visual models from natural language supervision. URL https://arxiv.org/abs/2103.00020v1.

Alexander Robey, George J. Pappas, and Hamed Hassani. Model-based domain generalization. In *Thirty-Fifth Conference on Neural Information Processing Systems*, 2021. URL https://openreview.net/forum?id=JOxB9h40A-1.

Sara Sabour, Nicholas Frosst, and Geoffrey E. Hinton. Dynamic routing between capsules. In *Proceedings of the 31st International Conference on Neural Information Processing Systems*, NIPS'17, pp. 3859–3869, Red Hook, NY, USA, 2017. Curran Associates Inc. ISBN 9781510860964.

J. Stillwell. *Naive Lie Theory*. Undergraduate Texts in Mathematics. Springer New York, 2008. ISBN 9780387782157. URL https://books.google.fr/books?id=SuR5OAgxyDIC.

Kai Sheng Tai, Peter Bailis, and Gregory Valiant. Equivariant Transformer Networks. In *International Conference on Machine Learning*, 2019.

Trimble Inc. 3d warehouse. https://3dwarehouse.sketchup.com/. Accessed: 2022-03-07.

Julius von Kügelgen, Yash Sharma, Luigi Gresele, Wieland Brendel, Bernhard Schölkopf, Michel Besserve, and Francesco Locatello. Self-supervised learning with data augmentations provably isolates content from style. 2021. URL http://arxiv.org/abs/2106.04619.

Ross Wightman. Pytorch image models. https://github.com/rwightman/pytorch-image-models, 2019.

Kaiyang Zhou, Yongxin Yang, Timothy M. Hospedales, and Tao Xiang. Deep domain-adversarial image generation for domain generalisation. In *The Thirty-Fourth AAAI Conference on Artificial Intelligence, AAAI 2020, The Thirty-Second Innovative Applications of Artificial Intelligence Conference, IAAI 2020, The Tenth AAAI Symposium on Educational Advances in Artificial Intelligence, EAAI 2020, New York, NY, USA, February 7-12, 2020*, pp. 13025–13032. AAAI Press, 2020. URL https://aaai.org/ojs/index.php/AAAI/article/view/7003.

Roland S. Zimmermann, Yash Sharma, Steffen Schneider, Matthias Bethge, and Wieland Brendel. Contrastive learning inverts the data generating process. 139:12979–12990, 2021. URL http://proceedings.mlr.press/v139/zimmermann21a.html.

A Background: matrix Lie groups

Group action definition If G is a group with identity element e, and $\mathcal{Z}$ is a set, then a group action ϕ is a function $\phi : G \times \mathcal{Z} \to \mathcal{Z}$ such that the following conditions hold:

1. $\phi(e, z) = z$

2. $\phi(g_1, \phi(g_2, z)) = \phi(g_2 g_2, z) \forall g_1, g_2 \in G$

The action ϕ is a left-group action in this case.

Matrix Lie groups Lie groups are continuous groups described by a set of real parameters (Hall, 2003). A matrix Lie group G is a *closed* subgroup of the general linear group $\mathrm{GL}(m, \mathbb{C})$ (the set of invertible complex matrices of size m), with matrix multiplication as group operation. Furthermore, if G is connected, then we can continuously traverse its elements.

Interestingly, many continuous transformations form matrix Lie groups. However, matrix Lie groups lack the typical structure of a vector space. For example adding two rotation matrices does not produce a rotation matrix. For each matrix Lie group however, there's a corresponding Lie algebra $\mathfrak{g}$ which is the tangent space of the group G at the identity. A Lie algebra forms vector space where addition is a closed operation and where the space can be described using basis matrices. Using the matrix exponential $\exp : \mathfrak{g} \to G$, the Lie algebra is the set of all matrices $\mathbf{M}$ such that $\exp(t\mathbf{M}) \in G$ for all real numbers t. If G is connected, then every element of G can be expressed as a product of exponential of elements of the Lie algebra. If we further assume that G is connected and compact, the exponential map is surjective i.e. every element of the group can be expressed as a single exponential of an element of the Lie algebra.

We refer the reader to (Hall, 2003; Stillwell, 2008) for a more detailed presentation of Lie algebra of matrix Lie groups.

B Experimental details

B.1 Training details

Generalization gaps for SoTA vision models To measure the generalization gaps of SoTA vision models, we use ImageNet pre-trained models (with the exception of CLIP). For SimCLR we use the pretrained model available on PyTorch Lightning Bolts. For CLIP, we use the pretrained CLIP model available from Hugging Face Transformers. For ViT, we use the pretrained model available in Timm Wightman (2019). For MAE we use the weights and model architecture available from the official repo. For VICReg, we use the weights and model architecture available from the the official repo. For supervised linear evaluation, we train all models for 100 epochs across 7 logarithmically scaled learning rates between 1e-1 and 1-6 using both sgd and Adam with a batch size of 32. We finetune models using the same setup with 7 logarithmically scaled learning rates

between 1e-2 and 1e-6. We then evaluate models trained in both setups by measuring the gap between the Top-1 accuracy of training instances in the typical pose and diverse poses in 2.

Lie models and their baselines   For MAE/VICReg Lie and their baselines we also use ImageNet pre-trained models. For the self-supervised finetuning phase, we train models for 100 epochs followed by supervised finetuning or linear evaluation of 10,000 or 20,000 steps respectively. During the self-supervised phase, all models are trained on data where half of the instances are seen undergoing pose changes. During the supervised training phases, we vary this proportion and show performance results in the main paper.

Computation   : We find our Lie models achieved comparable runtimes on 8 GPUs relative to the baselines for the self-supervised training phase of approximately 2 hours for MAE Lie and 3 hours on VICReg Lie. The overall compute required for the self-supervised phase experiments consisted of the sweeps described in Appendix B.1.2 of approximately 75 runs each requiring 2-3 hours of training on 8 GPU machines. We did find using Option 2 during supervised training (see Appendix B.1.1), to increase runtime since this requires sampling t and computing a full matrix exponential for each sample (e.g., approximately 2.5 hours for linear eval on VICReg Lie versus 1.5 hours for VICReg).

B.1.1   Architectures

Storing and re-using learned t in the context of Lie models   During the Lie models supervised linear eval or finetuning, we access single images (and not pairs). The supervised classifier uses the Lie backbone to which the single image is fed. At this point we tried two options. Option 1 is to simply retrieve the representation vector $\mathbf{z}$ from the Lie encoder, as with any other baseline model. Option 2 is to use the learned Lie operators to generate "neighbors", that are, transformed versions of that image (represented in embedding space). The intuition behind this option is that we use the Lie generators to create artificial, transformed images (the neighbors of the initial sample) and average the losses over these to increase these neighbors images to improve invariance of the classifier with respect to pose changes.

For Option 2 during training, once the image is fed to the Lie encoder, we generate the representation vector $\mathbf{z}$ for that image but also "neighbors" by (i) sampling random $\mathbf{t}_1, ..., \mathbf{t}_k$ vectors (ii) computing the corresponding $\hat{g}_1, ..., \hat{g}_k$ as in Step 3 of Algorithm 1 (iii) and computing corresponding neighbors $\mathbf{z}^{\hat{g}_1}, ..., \mathbf{z}^{\hat{g}_k}$ as in Step 4 of 1. We consider these the "neighbors" of $\mathbf{z}$, which represent transformed version of the image, but in the embedding space. Then, if we're in training stage, we back-propagate the loss of the classifier on all neighbors. If we're in evaluation / testing stage, we perform the prediction on the image and don't use the neighbors.

We explored both options in our initial experiments and found that they made lit-

tle difference. Hence, we report MAE Lie and VICReg Lie using Option 2 with 1 neighbor.

Architecture for inferring t To infer t from the ground truth δ we use a multi-layer perceptron with two linear layers connected by a leaky ReLU. The inference network takes as inputs δ and the two embeddings. The network outputs a t matching the dimension of the Lie algebra * batch dimension.

B.1.2 Lie hyperparameter sweeps

MAE Lie sweep: For MAE Lie and its MAE baseline we use a similar procedure. For the self-supervised learning phase, models are trained with a batch size of 64 for 100 epochs. We sweep over three learning rates 5e-4,5e-5,5e-6 using the Adam optimizer along with every combination of each λ in $\{1, 5\}$. The baseline MAE model is trained with λ_{lie} and λ_{euc} set to zero. To cross validate, we use validation accuracy with the same diversity proportion as in training. For the supervised phase, we sweep over learning rates of 5e-3,5e-4,5e-5,5e-6 for finetuning and 5e-3,5e-4,5e-5 for linear evaluation. We show results for the best set of hyperparameters selected based on combined validation accuracy, which samples both diverse and typical poses for instance to match those seen during training. We report the average and standard errors of Top-1 accuracy across three seeds.

VICReg Lie sweep: The procedure for VICReg Lie is similar to MAE Lie, small difference is that we use every combination of each λ in $\{0, 1, 5\}$. The baseline VICReg model is trained with λ_{lie} and λ_{euc} set to zero.

B.1.3 Transfer experiments

For the experiments in Section 5, we finetune both the baseline MAE model and MAE Lie for 20k steps on ImageNet with a linear classification head. We sweep over the following learning rates $5e - 4, 5e - 5, 5e - 6$ with a batch size of 64 when finetuning each model. We select the best model based on the validation loss.

C Code and data

We base our data generation code on https://github.com/panmari/stanford-shapenet-renderer. We use 52 classes for our analysis after omitting 3 classes which contain overlapping instances. We select 50 instance from each class and partition those into 10% for validation and 15% for testing. For instance show in diverse poses, we show all possible pose configurations in 2D and 3D with a step size of 4 degrees. For 3D rotation we set the angles of all three axes to the same value. The resulting dataset consists of 500,000 unique images. Figure A1 shows a sample of instance images in various poses across five classes.

Figure A1: **Sample images of the shapes dataset in various 2D and 3D poses**. From the upper left onward is class guitar, lamp, birdhouse, plant, and plane. The first image for each class is the canonical pose followed by 4, 8, 16, 32, 64, 128, 256 planar and 3D rotations. The last image for each class is (320, 320, 320) degree 3D pose. In our training and evaluation, we use full span of 2D and 3D pose change with a step size of 4 degrees.
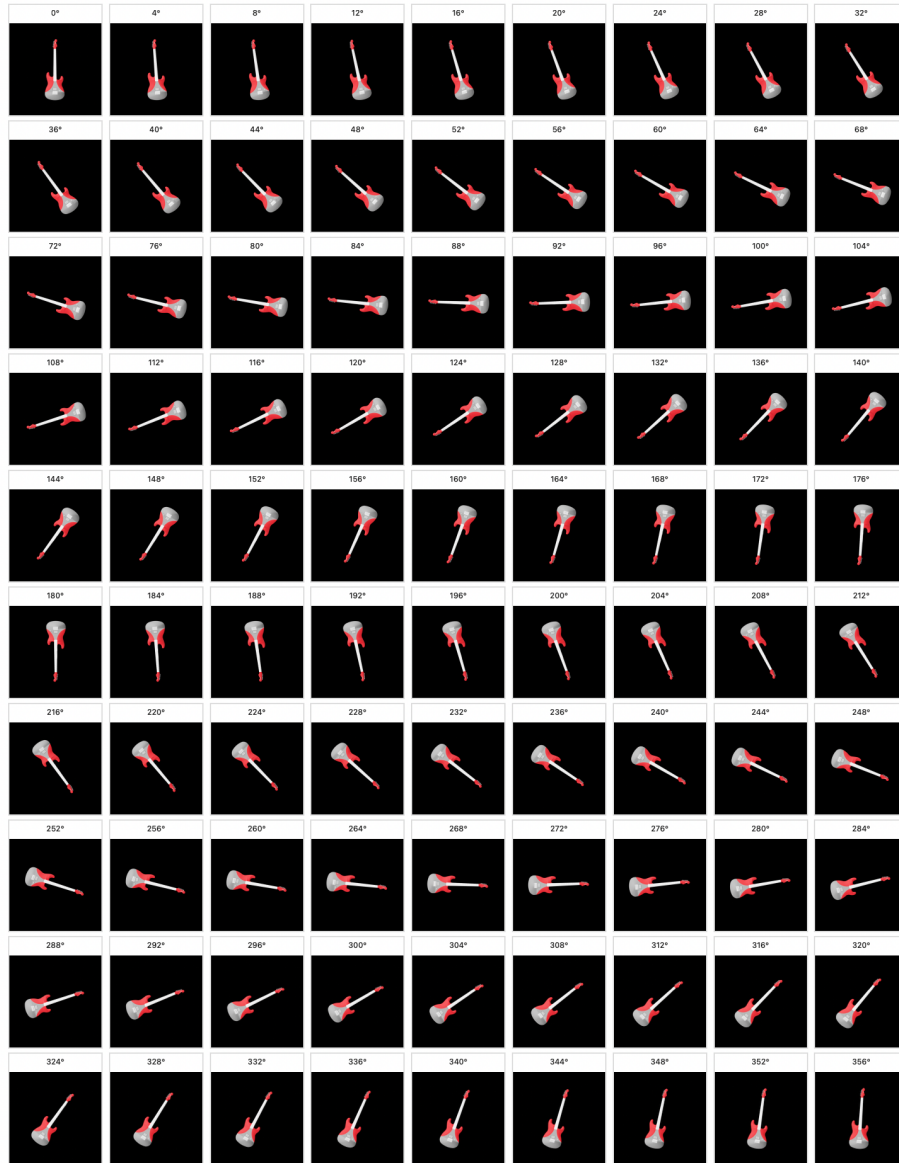
Figure A2: **Guitar object instance in all 2D pose configurations.** The poses vary by a step size of 4 degrees with the pose angle of each image shown above.

Figure A3: **Guitar object instance in all 3D pose configurations.** The poses vary by a step size of 4 degrees with the pose angle of each image shown above.

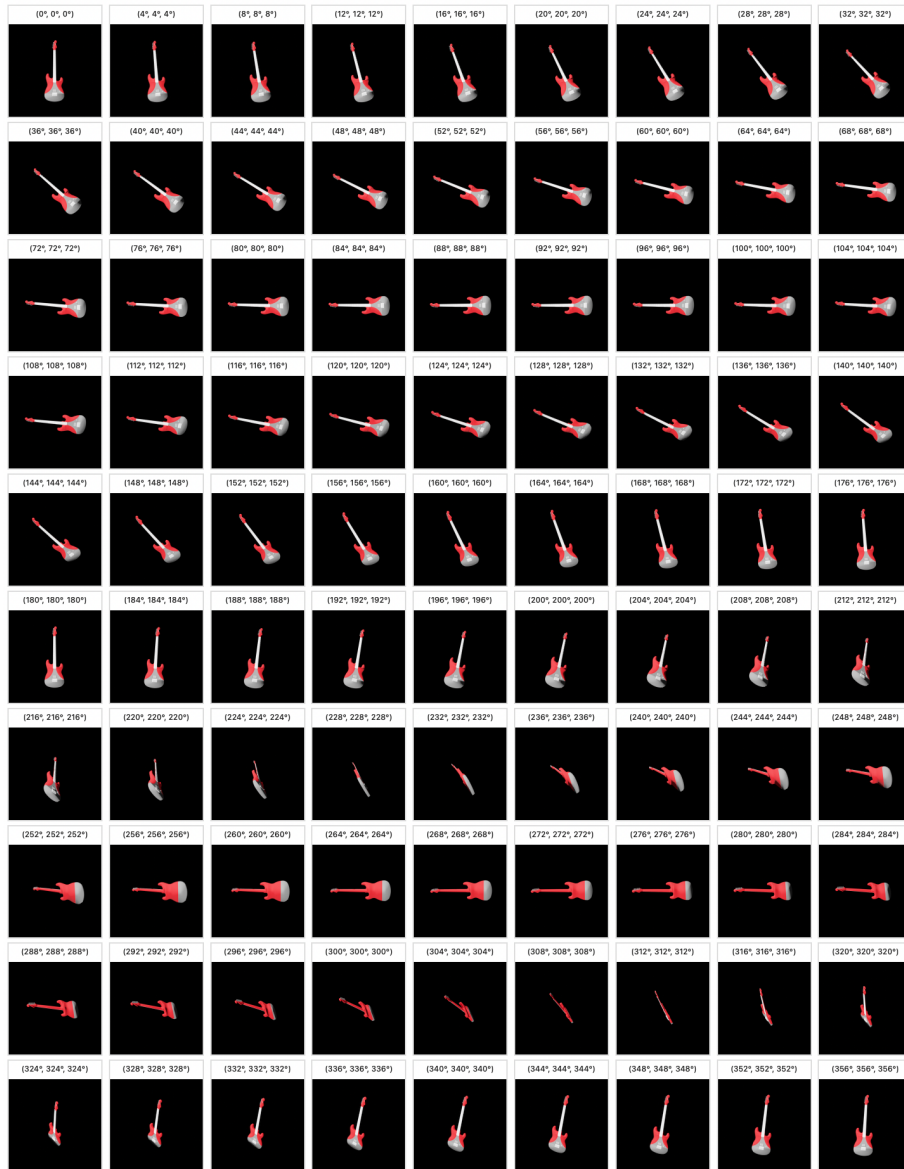# D   Additional Results

D.1   Pose changes in 3D

We show additional results for MAE Lie and VICReg Lie for 3D pose changes in Table A1 and A2.

Table A1: **Linear evaluation performance for 3D pose changes as the proportion of diverse instances seen during training varies.** Table reports linear evaluation top-1 accuracy as **mean** $\pm$ standard error (**+ absolute difference, x relative multiple**) to the baseline model.

	known instance in new pose			unknown instance		
diverse proportion	0.05	0.25	0.50	0.05	0.25	0.50
MAE Lie	12.3 ± 0.3 (**+3.0, 1.32x**)	12.1 ± 0.4 (**+3.1, 1.35x**)	14.9 ± 0.3 (**+4.8, 1.48x**)	11.8 ± 0.3 (**+3.1, 1.35x**)	10.5 ± 0.4 (**+2.0, 1.24x**)	12.1 ± 0.2 (**+2.6, 1.28x**)
MAE	9.4 ± 0.1	8.9 ± 0.4	10.1 ± 0.3	8.7 ± 0.1	8.5 ± 0.2	9.4 ± 0.6
VICReg Lie	65.0 ± 0.1 (**+11.3, 1.21x**)	68.5 ± 0.0 (**+4.3, 1.07x**)	72.8 ± 0.1 (**+5.7, 1.09x**)	51.3 ± 0.1 (**+4.7, 1.10x**)	57.4 ± 0.1 (**+2.2, 1.04x**)	59.6 ± 0.1 (**+0.9, 1.02x**)
VICReg	53.7 ± 0.0	64.2 ± 0.1	67.1 ± 0.1	46.6 ± 0.1	55.2 ± 0.1	58.7 ± 0.2

Table A2: **Finetuning performance for 3D pose changes as the proportion of diverse instances seen during training varies.** Table reports linear evaluation top-1 accuracy as **mean** $\pm$ standard error (**+ absolute difference, x relative multiple**) to the baseline model.

	known instance in new pose			unknown instance		
diverse proportion	0.05	0.25	0.50	0.05	0.25	0.50
MAE Lie	43.2 ± 0.1 (**+8.6, 1.25x**)	54.9 ± 0.0 (**+12.8, 1.31x**)	59.5 ± 0.4 (**+13.9, 1.31x**)	26.3 ± 0.2 (**+7.6, 1.40x**)	35.3 ± 0.0 (**+11.4, 1.48x**)	39.3 ± 1.0 (**+12.1, 1.44x**)
MAE	34.6 ± 0.2	42.0 ± 0.3	45.6 ± 0.6	18.8 ± 0.2	23.9 ± 0.3	27.2 ± 0.4

E   Applying the Lie operator to SimCLR (Chen et al., 2020)

We also experiment applying our Lie operator to the SimCLR architecture (Chen et al., 2020), where L_{ssl} is the regular SimCLR Loss. Since the Lie models receive frame pairs as input, we construct an additional baseline, SimCLR Frames, with access to the same pairs of frames. In addition to the standard InfoNCE loss for SimCLR we add an additional InfoNCE loss to encourage similarity in the embeddings of the two frames. This baseline accounts for any performance gain simply due to the extra organization found by pairing frames. We report results of SimCLR, SimCLR Frames, and SimCLR Lie in Tables A3, A4, A6 A6. Across all evaluation settings, we find our Lie operator extension of SimCLR matches or outperforms SimCLR Frames and SimCLR baselines, with best gains in the linear evaluation setting.

SimCLR Training details   We developed SimCLR Lie early in our experimental study, and explain here the procedure for training. In the case of SimCLR Lie for self-

Table A3: **SimCLR Lie versus baselines: Linear evaluation robustness to pose changes as the proportion of diverse instances seen during training varies.** Table reports linear evaluation top-1 accuracy as **mean** $\pm$ standard error (+ absolute difference, x relative multiple) to the baseline model.

diverse proportion top-1 accuracy (%)	known instance in new pose			unknown instance		
	5%	25%	50%	5%	25%	50%
SimCLR Lie	**56.0 ± 0.2 (+5.8, 1.12x)**	**65.4 ± 0.1 (+3.4, 1.05x)**	**70.0 ± 0.1 (+4.0, 1.06x)**	**45.7 ± 0.1 (+2.6, 1.06x)**	**56.0 ± 0.1 (+1.7, 1.03x)**	**59.0 ± 0.2 (+0.8, 1.01x)**
SimCLR	50.2 ± 0.3	62.0 ± 0.1	66.0 ± 0.1	43.0 ± 0.3	54.3 ± 0.0	58.3 ± 0.2
SimCLR Frames	49.1 ± 0.2	60.6 ± 0.1	65.2 ± 0.0	42.2 ± 0.2	53.3 ± 0.1	58.0 ± 0.0

Table A4: **SimCLR Lie versus baselines: Finetuning robustness to pose changes as the proportion of diverse instances seen during training varies.** Table reports finetuning Top-1 Accuracy as **mean** $\pm$ standard error (+ absolute difference, x relative multiple) to the baseline model.

diverse proportion top-1 accuracy (%)	known instance in new pose			unknown instance		
	5%	25%	50%	5%	25%	50%
SimCLR Lie	**55.1 ± 0.4 (+0.9, 1.02x)**	**65.9 ± 0.6 (+1.2, 1.02x)**	**70.9 ± 0.4 (+0.7, 1.01x)**	**45.9 ± 0.1 (+0.5, 1.01x)**	**55.9 ± 0.2 (-0.0, 1.00x)**	**61.8 ± 0.8 (+0.7, 1.01x)**
SimCLR	54.2 ± 0.8	64.7 ± 0.2	70.2 ± 0.2	45.4 ± 0.3	56.0 ± 0.2	61.1 ± 0.4
SimCLR Frames	53.9 ± 0.2	64.8 ± 0.6	70.7 ± 0.2	45.2 ± 0.2	55.8 ± 0.1	61.8 ± 0.5

Table A5: **SimCLR Lie versus baselines: Linear evaluation performance for 3D pose changes as the proportion of diverse instances seen during training varies.** Table reports linear evaluation top-1 accuracy as **mean** $\pm$ standard error (+ absolute difference, x relative multiple) to the baseline model.

diverse proportion	known instance in new pose			unknown instance		
	0.05	0.25	0.50	0.05	0.25	0.50
SimCLR Lie	**50.9 ± 0.1 (+4.5, 1.10x)**	**61.0 ± 0.1 (+2.4, 1.04x)**	**64.7 ± 0.1 (+2.7, 1.04x)**	**43.2 ± 0.1 (+2.4, 1.06x)**	**53.6 ± 0.1 (+0.9, 1.02x)**	**56.2 ± 0.1 (+0.4, 1.01x)**
SimCLR	46.4 ± 0.2	58.6 ± 0.1	61.9 ± 0.2	40.8 ± 0.3	52.8 ± 0.1	55.8 ± 0.2
SimCLR Frames	45.6 ± 0.2	57.4 ± 0.1	61.0 ± 0.1	40.0 ± 0.2	51.2 ± 0.1	55.4 ± 0.1

Table A6: **SimCLR Lie versus baselines: Finetuning performance for 3D pose changes as the proportion of diverse instances seen during training varies.** Table reports linear evaluation top-1 accuracy as **mean** $\pm$ standard error (+ absolute difference, x relative multiple) to the baseline model.

diverse proportion	known instance in new pose			unknown instance		
	0.05	0.25	0.50	0.05	0.25	0.50
SimCLR Lie	**49.6 ± 0.5 (+1.0, 1.02x)**	**62.3 ± 0.2 (+0.4, 1.01x)**	**66.9 ± 0.3 (+0.1, 1.00x)**	**42.0 ± 0.3 (+0.8, 1.02x)**	**54.2 ± 0.2 (-0.7, 0.99x)**	**59.8 ± 0.5 (-0.2, 1.00x)**
SimCLR	48.6 ± 0.5	61.9 ± 0.4	66.8 ± 0.2	41.3 ± 0.6	54.9 ± 0.1	60.1 ± 0.3
SimCLR Frames	48.7 ± 0.4	62.2 ± 0.5	67.3 ± 0.1	41.5 ± 0.2	55.1 ± 0.5	59.7 ± 0.5

supervised learning phase, we cross-validated using top 1 online validation combined accuracy but we filter models such that the validation L_{Lie} loss, evaluated on the 2D rotated validation set, at the last epoch, is 60% smaller or equal to its first epoch's value. We found that online validation combined accuracy was not enough as a metric to shed light on the behavior of our Lie model on the representational space and do this filtering to ensure that the Lie operator bring the transformed sample close to its target. Also, note that in linear evaluation and finetuning, we report SimCLR Lie using Option 1 (regular supervised training of the classifier). For self-supervised learning phase:

- We cross-validate with $\lambda_{\mathrm{lie}} \in \{1, 5, 10\}, \lambda_{\mathrm{ssl}} \in \{1, 5, 10\}, \lambda_{\mathrm{euc}} \in \{1, 2\}$. Best hyper-parameters chosen with the cross-validation procedure explained is $\lambda_{\mathrm{lie}} = 10, \lambda_{\mathrm{ssl}} = 10, \lambda_{\mathrm{euc}} = 1$.

- We cross-validate with learning rates in $5e - 5, 5e - 6$.

For supervised linear evaluation:

- We cross-validate with learning rates in $5e - 3, 5e - 4, 5e - 5$.

For supervised finetuning:

- We cross-validate with learning rates in $5e - 3, 5e - 4, 5e - 5, 5e - 6$.